

# Structural-Phase Changes in Oxidized Alloy Zr-1%Nb, Induced by Irradiation with High-Intensive Beams of Nitrogen Ions

T.A. Belykh, N.V. Gavrilov, O.A. Golosov\*, D.R. Emlin, M.V. Kuznetsov\*\*,  
A.M. Murzakaev, L.P. Sinelnikov\*, A.N. Timokhin\* and A.G. Trifanov\*

*Institute of Electrophysics UD RAS, 106 Amundsen St., Ekaterinburg, 620016, Russia*

*Phone: (343)267 87 78, fax (343)267 87 94, e-mail: pulsar@jep.uran.ru*

*\*Institute of Reactor Materials, Mail Box 29, Zarechny, 624250, Russia*

*\*\*Institute of Solid State Chemistry UD RAS, 91 Pervomaiskaya St., Ekaterinburg, 620219, Russia*

**Abstract** – It was analyzed how a nitrogen ion beam influenced corrosion resistance of an oxidized Zr-1% Nb alloy. The study revealed optimal regimes of ion implantation leading to the decrease in the rate of both general and pitting corrosion. Structural and phase transformations induced by ion implantation were analyzed by X-ray photoelectron spectroscopy and scanning electron microscopy.

## 1. Introduction

Zr-Nb alloys are widely used in the nuclear reactor industry [1]. Traditional anticorrosion technologies based on preliminary formation of surface oxide layer fail to prolong the lifetime of products. Since nitrogen impurity in zirconium accelerates the corrosion rate [2], it would be reasonable to modify the  $ZrO_{2-x}/Zr-Nb$  heterostructure rather than the alloy [3]. It was shown [4] that irradiation of passivating oxide layers with high-current beams of nitrogen ions decelerated general corrosion. In addition to general corrosion, zirconium alloys are prone to point or pitting corrosion, which is characterized by high oxidation rate of local surface areas. Most frequently, it is this type of corrosion that determines the lifetime of products. Since both types of corrosion are sensitive to the structure and the composition of the alloy, the objective of the study was to analyze the effect of ion implantation regimes on the structural and phase state of the surface layer and the rate of corrosion.

## 2. Experimental Technique

Subjects of study were samples of the Zr-1% Nb alloy with an oxide layer of  $ZrO_{2-x}$  about 0.2  $\mu m$  thick, which was produced using a standard oxidation technology.

A pulsed repetitive source of ions [5] served for modification of properties of the  $ZrO_{2-x}/Zr-Nb$  heterostructure. The working gas was nitrogen. The accelerating voltage was 30 kV, the beam current density was 3 mA/cm<sup>2</sup>, the pulse length was 1 ms, and the pulse repetition frequency was 3–25 Hz. The working gas pressure in the vacuum chamber was equal to 4–6·10<sup>-2</sup> Pa. Temperature of the samples, which was de-

termined by the ion beam power and conditions of additional forced heating, varied between 50 and 400 °C.

The samples were exposed to N<sup>+</sup> beams with a fluence of 10<sup>15</sup> to 10<sup>18</sup> cm<sup>-2</sup> and then were subject to corrosion tests including “afteroxidation” in an electric resistive furnace at 400 °C in air. The temperature was maintained to within  $\pm 2^\circ$ . The corrosion rate was indexed by the overweight, that is, the increase in the sample weight referred to a unit area (mg/cm<sup>2</sup>). The samples were weighed on a VLD-20 laboratory scale having the accuracy of 5·10<sup>-6</sup> g. Proneness of the samples to point corrosion was tested in a solid electrolyte (Ni + Li<sub>2</sub>O powder) during 50 hours at 520 °C.

The chemical state of elements in surface layers of zirconium dioxide before and after implantation of nitrogen ions was analyzed by X-ray photoelectron spectroscopy (XPS) using an ESCALAB MK II electron spectrometer. Photoemission of electrons from core and valence states was excited by nonmonochromatic Al K <sub>$\alpha$</sub>  radiation ( $E_{hv} = 1486.6$  eV). The XPS analysis depth was 3–5 nm. To watch changes in the phase composition at a depth down to 120 nm, the samples were etched using an argon ion beam with an energy of 6 keV and a current of 20  $\mu A$ .

The surface morphology of the samples before and after implantation was examined by scanning electron microscopy in a LEO 982 microscope.

## 3. Results and Discussion

Figure 1 presents kinetic curves of the weight increment for samples subjected to implantation at a temperature of 400 °C, which corresponded to a maximum retardation of general corrosion equal to ~20%. The oxidation kinetics had a two-stage form characteristic of zirconium: a parabolic dependence at a small depth of the oxide layer and a linear dependence after the inflection point.

The photographs in Fig. 2 show samples tested for proneness to point corrosion. Areas affected by point corrosion were detected on reference template samples and samples subjected to implantation at temperatures below 300 °C and fluences smaller than 10<sup>17</sup> cm<sup>-2</sup>. Point corrosion could not be induced in samples

Nos. 62 and 58, which were subject for implantation at fluences of  $10^{17}$  and  $10^{18}$   $\text{cm}^{-2}$  and a temperature of 400 °C.

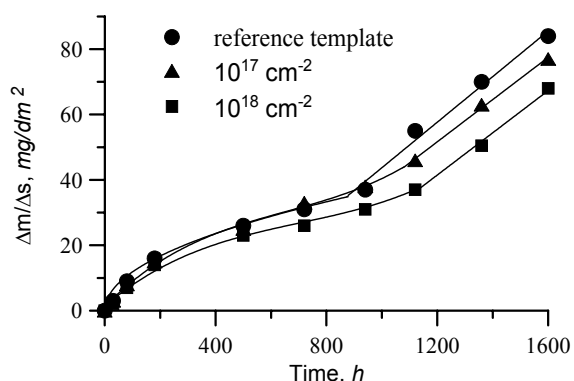


Fig. 1. Oxidation kinetics of samples after implantation of nitrogen ions at 400 °C

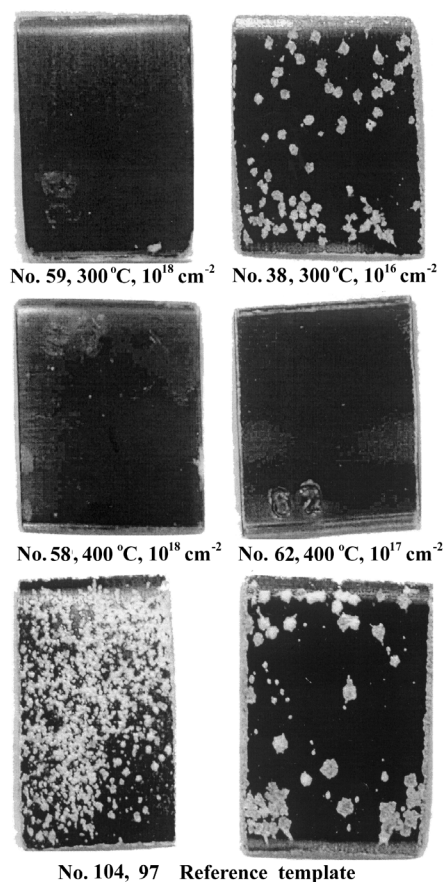


Fig. 2. External appearance of samples after they were tested for proneness to point corrosion

Table 1 gives data for a specific surface damaged by point corrosion. The data was obtained from processing of images using the SIAMS program. As the implantation temperature was elevated to 400 °C and the fluence increased up to  $10^{17}$   $\text{cm}^{-2}$  or higher, the area affected by point corrosion diminished from 20–30% to 0.1–0.2%. Considerable improvement of corrosion properties of the test samples was due probably to structural and phase changes caused by implantation.

Table 1

№ samples	The parameters of implantation		The area affected by point corrosion diminished, %
	T, °C	fluens, $\text{cm}^{-2}$	
12	50	$10^{15}$	33.3
4		$10^{16}$	4.8
26	200	$10^{15}$	13.9
18		$10^{16}$	9.25
16		$10^{17}$	11.8
70		$10^{18}$	2.45
38		$10^{16}$	12.4
59	300	$10^{18}$	7.95
62	400	$10^{17}$	0.25
58		$10^{18}$	0.15
97	Reference template		20.25
104	Reference template		30.55

The XPS analysis revealed additional phases, which appeared after implantation. Fig. 3 presents XPS spectra, from which it follows that inclusions of  $\text{ZrN}_x\text{O}_y$  oxynitride phases and lower metastable  $\text{Zr}_2\text{O}_3$  oxides appeared after implantation at fluences of  $10^{17}$   $\text{cm}^{-2}$  and higher.

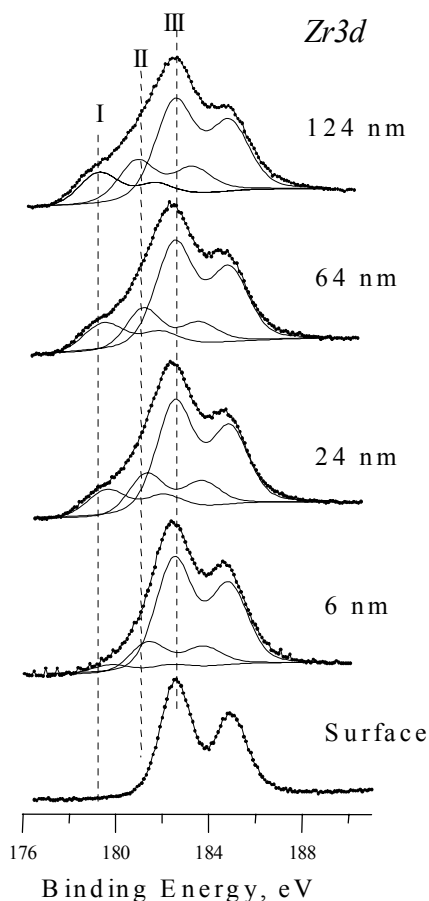


Fig. 3. Intensity of XPS lines in Zr3d spectra of the oxidized Zr-1% Nb alloy after exposure to nitrogen ions with a fluence of  $10^{17}$   $\text{cm}^{-2}$  versus depth: I –  $\text{ZrN}_x\text{O}_y$ ; II –  $\text{Zr}_2\text{O}_3$ ; III –  $\text{ZrO}_2$

The maximum of the line I of the Zr3d XPS spectrum resolution, which corresponded to the  $\text{ZrN}_x\text{O}_y$  phase, was located at a depth nearly equal to the pro-

jective path of nitrogen ions having energy of 30 keV. The formed layer of oxynitride phase precipitates could serve as a getter of structural defects and impurities.

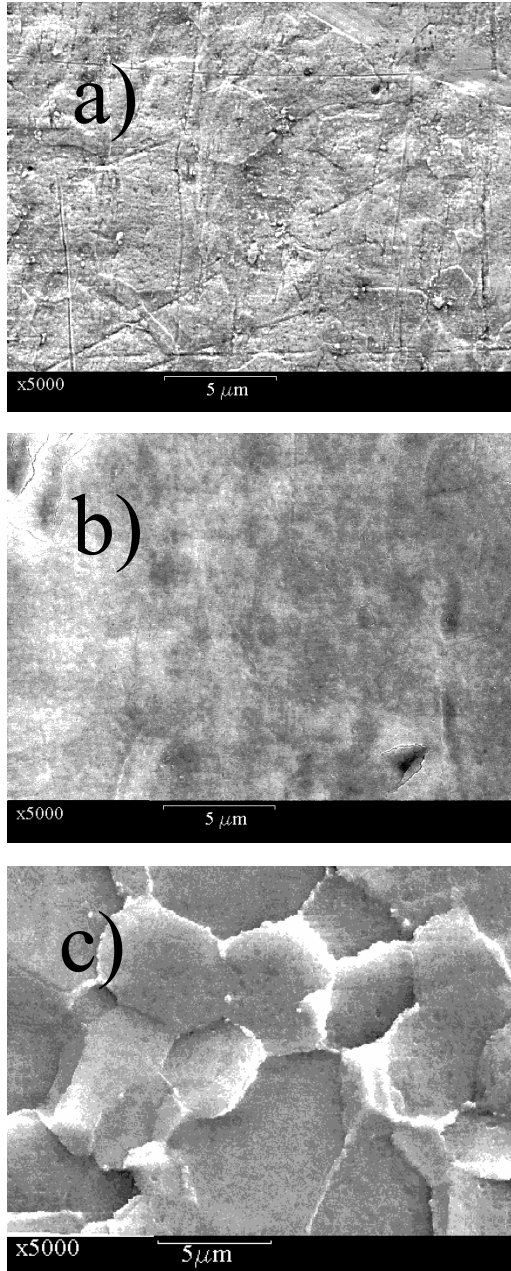


Fig. 4. Surface microstructure of oxidized Zr-1% initial (a); after irradiation at 400 °C (b); after irradiation at 500 °C (c) (5000 x)

In addition to the chemical action (implantation of nitrogen and precipitation of new phases), implantation had a physical effect thanks to dissipation of the energy of ion beam. The power released by the beam could induce structural rearrangements of the target material. Fig. 4 depicts electron microscopic images of the surface of test samples in the initial state and after implantation of nitrogen ions at a fluence of

$10^{18} \text{ cm}^{-2}$  and an average implantation temperature of 400 °C and 500 °C. The film on the initial sample (Fig. 5, a) had different thickness (50000 x magnification), a loose structure and traces of mechanical treatment (Fig. 4, a, 5000 x). Looseness of the initial film was detected in our earlier studies [4], which revealed the presence of H<sub>2</sub>O and unbound nitrogen in the film.

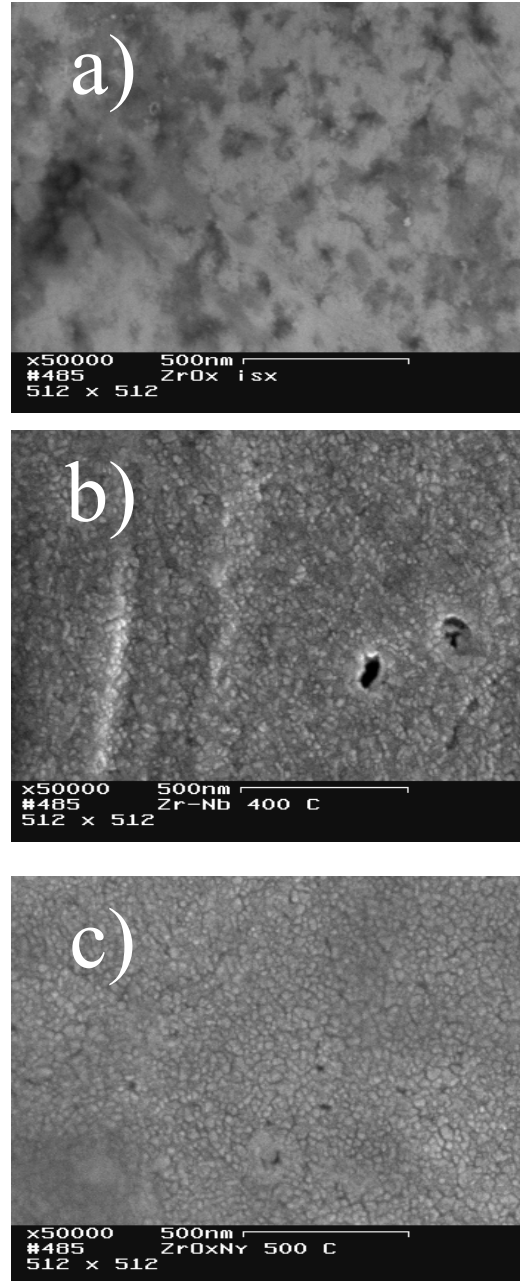


Fig. 5. Surface microstructure of oxidized Zr-1% initial (a); after irradiation at 400 °C (b); after irradiation at 500 °C (c) (50000 x)

The author [6] also noted that the structure of ZrO<sub>2-x</sub> oxides, which were prepared by oxidation of zirconium, had numerous pores. Having a characteristic hexagonal shape (Fig. 4, c, 5000 x) appeared as the average implantation. Implantation led to homogeni-

zation of the film (Fig. 5, b): its surface smoothed; a texture of crystallites about 20–30 nm in size was obvious; small defects resulting from mechanical treatment were eliminated. A rough surface with crystallites temperature increased up to 500 °C. This was an indication that exposure to high-intensity beams caused polymorphous transformation from the initial low-temperature monoclinic structure to a high-temperature tetragonal structure. The inner texture of crystallites was preserved (Fig. 5, c, 50 000 x). Corrosion properties of the film in this new state will be the subject of future studies.

#### 4. Conclusion

Thus, treatment with high-intensity beams of nitrogen ions caused structural and phase rearrangement in surface layers of  $ZrO_{2-x}$ , which improved corrosion resistance of  $ZrO_{2-x}/Zr-1\%$  Nb heterostructures. Implantation at an average temperature of samples equal

to 400 °C and ion radiation fluences of  $10^{17}$ – $10^{18}$   $cm^{-2}$  is optimal for passivation of Zr-Nb alloys.

#### References

- [1] A.S. Zaimanovsky, A.V. Nikulina, N.G. Reshetnikov, *Zirconium Alloys in Atomic Power Engineering*, Moscow, Energoatomizdat, 1981, 232 pp.
- [2] R.F. Voitovich, *Oxidation of Zirconium and its Alloys*, Kiev, Naukova Dumka, 1989, 288 pp.
- [3] A.V. Matveev, T.A. Belykh, V.I. Perekhozhev et al., A Method for Treatment of Zirconium Alloys. *Patent for Invention No. 2199607* dated February 27, 2003.
- [4] T.A. Belykh, A.V. Gavrilov, O.A. Golosov et al., FCOM, No. 6, 14–20 (2003).
- [5] N.V. Gavrilov, S.P. Nikulin, G.V. Radkovsky, PTE, No. 1, 93–98 (1996).
- [6] O.A. Alekseev, *Atomnaya Energetika za Rubezhom*, No. 2, 30–35 (1981).